Available online at www.sciencedirect.com
ScienceDirect
Journal of Sound and Vibration 321 (2009) 342–362
JOURNAL OF SOUND AND VIBRATION
www.elsevier.com/locate/jsvi

Thermo-mechanical vibration of FGM sandwich beam under variable elastic foundations using differential quadrature method

S.C. Pradhan*, T. Murmu

Department of Aerospace Engineering, Indian Institute of Technology, Kharagpur, West Bengal 721 302, India

Received 19 November 2007; received in revised form 23 April 2008; accepted 11 September 2008
Handling Editor: L.G. Tham
Available online 23 October 2008

Abstract

Thermo-mechanical vibration analysis of functionally graded (FG) beams and functionally graded sandwich (FGSW) beams are presented. The functionally graded material (FGM) beams are considered to be resting on variable (i) Winkler foundation and (ii) two-parameter elastic foundation. The material properties of these beams are assumed to be varying in the thickness direction. The governing differential equations for beam vibration are being solved using the modified differential quadrature method (MDQM). The applied kinematic boundary conditions are implemented using the modified weighting coefficient matrix (MWCM). The weighting coefficients are generated from the Chebyshev basis function. Present results for the vibration of isotropic beam with variable Winkler foundation are in good agreement with those reported in the literature. Parametric study on the vibration response of FG beams and FGSW beams are being investigated. These parameters include (i) temperature distributions, (ii) power-law index, (iii) variable Winkler foundation modulus, (iv) two-parameter elastic foundation modulus and (v) normalized core thickness of FGSW beams.

1. Introduction

Functionally graded (FG) structures are found in space vehicles, aircrafts, automobiles, nuclear power plants, combustion chambers and turbine blades, etc. These structures are often subjected to vibration with thermal and dynamic loadings. The loadings include large temperature gradients, thermo-elastically induced loading and dynamic pressure. For example, in space shuttle, during re-entry into the earth's atmosphere, functionally graded material (FGM) tiles are utilized as heat shields. These tiles are made up of ceramic and metal and thus provide simultaneously thermal protection and load-carrying capability. FGMs are also used as a spacer for gas-insulated power equipment. Furthermore, ceramic–metal FGM are applied on the dual friction pair of green automobiles. Hence, it is important to study the structural response of FG structures under thermo-elastic loading.

*Corresponding author. Tel.: +91 3222 283008; fax: +91 3222 282242.
E-mail address: scp@aero.iitkgp.ernet.in (S.C. Pradhan).

0022-460X/$ - see front matter
doi:10.1016/j.jsv.2008.09.018

Nomenclature

A	cross-section area of beam
A_{ij},B_{ij},C_{ij},D_{ij}	first-, second-, third- and fourth-order weighting coefficients
A_{fgm}	in-plane stiffness of the FGM beam
B_{fgm}	bending–stretching coupling stiffness of the FGM beam
D_{fgm}	bending stiffness of the FGM beam
E_1,E_2	Young's moduli of materials 1 and 2
E_{fgm}	Young's modulus of FGM beam
h	thickness of FGM beam
k	Winkler elastic modulus
k_1	second parameter elastic modulus
k_{T1},k_{T2}	coefficients of thermal conductivity of materials 1 and 2
k_{fgm}	coefficient of thermal conductivity of FGM beam
L	length of beam
M	bending moment resultant of beam
n	no. of interpolation points
N	axial force resultant of beam
N_0	matrix of Chebyshev polynomial element
Rn	power-law index
Rt	core thickness ratio of sandwich beam
t	time variable
T	temperature
T(294–1500–294)	$T_1 = 294\,\mathrm{K}$, $T_2 = 1500\,\mathrm{K}$ and $T_3 = 294\,\mathrm{K}$
$T_n(x)$	nth Chebyshev polynomial of first kind
V_f	volume fraction of FGM beam
$W(x)$	mode shape of FGM beam
$w(x,t)$	deflection of beam
$x_0, x_1, .., x_n$	interpolation points
z	thickness coordinate

Greek letters

β	non-dimensional frequency parameter
ε_0	extensional strain
κ	bending strain
μ	sinusoidal variation parameter of elastic foundation
v_1,v_2	Poisson's ratios of materials 1 and 2
v_{fgm}	Poisson's ratio of FGM material
ξ	parabolic variation parameter of elastic foundation
ρ_1,ρ_2	densities of materials 1 and 2
ρ_{fgm}	density of FG material
ψ	linear variation parameter of elastic foundation
ω	natural frequency of beam
$\bar{\omega}$	non-dimensional natural frequency of beam

FGM have the properties that could vary in several suitable directions [1]. The mechanical properties of these materials are often being represented in the form of a series [2] and power-law index variations [3,4]. In these graded materials, there is a smooth and continuous variation of material properties across the thickness. This leads to no stress concentration and better fatigue life. Fundamental theories of FGM could be found in the paper of Suresh and Morton [5].

Various studies on FGM materials under thermo-mechanical environment are found in the literature. Praveen and Reddy [6] carried out thermo-elastic analysis of FG plates. They investigated the static and dynamic response of the FGM plates by varying the volume fraction of the ceramic and metallic constituents using the simple power-law distribution. Reddy and Cheng [7] studied the three-dimensional distribution of displacement and stresses of smart FG plates. Librescu et al. [8] studied the behavior of thin-walled beams made of FGM operating at high temperatures, which included vibration and instability analysis with effects of volume fraction, temperature gradients, etc. Review on various investigations of FGM including thermo-mechanical studies are found in Birman and Byrd [9].

Sandwich structures are often found in aerospace application such as in skin of wings, vertical fin torque box, aileron, spoilers, etc. The advantages of these structures are that it provides high specific stiffness and strength for a low-weight consideration. To maintain minimum weight for a given thermo-mechanical loading condition, FGM could be incorporated in the sandwich construction. Though there are research works reported on general sandwich structures, studies related to FGM sandwich (FGSW) structures are few in numbers. Li et al. [10] reported free vibration response of FGSW rectangular plates based on the three-dimensional elasticity theory. Their work included sandwich structures with FGM face sheet as well as with

FGM core. Zenkour [11] carried out stress analysis of FG ceramic–metal sandwich plates. Later Zenkour [12] reported buckling and vibration studies of sandwich plates. Venkataraman and Sankar [13] carried out analysis of sandwich beams with FG core where the face sheets were assumed to be isotropic and the core elastic coefficients were assumed to vary exponentially. The Euler–Bernoulli theory was employed for the analysis of face sheets.

The governing differential equations of FGM materials are solved by conventional methods. Sankar [14] obtained elasticity solution for simply supported functionally gradient beams subjected to sinusoidal transverse loading. In his paper, he developed a Euler–Bernoulli model of FG beam. Zhu and Sankar [15] used the Fourier-series-Galerkin method to obtain approximate solutions and computed displacements and stresses in a FG beam. Employing the finite element method, Chakroborty et al. [16] studied thermo-elastic effect and wave propagation in FGM beams. Zhong and Yu [17] carried out analytical work for a cantilever FGM beam. Bhangale and Ganesan [18] carried out thermo-elastic buckling and vibration behavior of FG sandwich beam using the finite element method.

Beam structures are often found to be resting on earth in various engineering applications. These include railway lines, geotechnical areas, highway pavement, building structures, offshore structures, transmission towers and transversely supported pipe lines. This motivated many researchers to analyze the behavior of beam structures on various elastic foundations.

Studies on homogenous isotropic beams resting on variable Winkler foundation are found in various papers. Zhou [19] studied vibration of a uniform single span beam resting on variable Winkler elastic foundation. Employing the finite element method, Thambiratnam and Zhuge [20] studied the free vibration analysis of beams resting on elastic foundations. Au et al. [21] considered a Euler–Lagrangian approach with C^1 continuity functions for the vibration and stability analyses of non-uniform beams resting on elastic foundation. For two-parameter elastic foundation, Matsunaga [22] studied the linear vibration of non-prismatic beams resting on two-parameter elastic foundations. Ying et al. [23] presented solutions for bending and free vibration of FG beams resting on a Winkler–Pasternak elastic foundation based on the two-dimensional theory of elasticity. However, works related to FGSW beam on variable Winkler foundation is limited in literature.

The differential quadrature method (DQM) is found to be a simple and efficient numerical technique for solving partial differential equations as reported by Bellman et al. [24]. Better convergence behavior is observed by DQM compared with its peer numerical competent techniques viz. the finite element method, the finite difference method, the boundary element method and the meshes less technique. Usually in these numerical techniques, accuracy improves with p, h and p–h refinements. However, in case of the present DQM technique, a smaller number of interpolation points are adequate to yield reasonably accurate results. In the present study, the Chebyshev polynomial of first kind [25] is employed in deriving the weighting coefficient matrix. For the imposition of boundary conditions of the structural problems, the delta method was originally employed by Bert et al. [26]. In this delta method, the boundary conditions are applied both at the beam boundaries and at a small distance 'delta' away from the boundaries. Though this implementation of boundary conditions is conceptually simple, this could not yield satisfactory results for boundary conditions other than the clamped–clamped boundary condition. Moreover, with very small 'delta' values, the results are found to be oscillating in nature. To remove the above drawback modified differential quadrature method (MDQM) approach is tried. Wang and Bert [27] employed a MDQM approach where all types of boundary conditions could be imposed exactly at the boundaries. In this new approach, during the formulation of weighting coefficients, the boundary conditions are incorporated. This approach is known as the modified weighting coefficient matrix (MWCM) method. Shu and Du [28] introduced the generalized differential quadrature (GDQ) method by substituting boundary conditions into the governing equations. It is found that MWCM yielded accurate results as compared with the delta method and the GDQ method for the same number of interpolation points. However with the GDQ method, clamped–clamped boundary condition is better handled. Though DQM is a simple and efficient numerical technique and has better convergence behavior, very few research work with MDQM application to the analysis of FGMs are available. Pradhan and Murmu [29] studied the flexural response of FG beams and sandwich structures using differential quadrature. They employed Chebyshev polynomial and the modified weight coefficient matrix method for determination of weighting coefficients and implication of boundary condition, respectively. Using the DQM, Fazelzadeh et al. [30] carried out vibration analysis of FG thin-walled rotating blades under high-temperature supersonic flow.

From the literature study, it is found that pure mechanical interaction of FGMs and elastic foundations is an important issue. This aspect is not being fully addressed in literature. Thus in the present paper, thermo-mechanical vibration analysis of FG beams and FGSW beams resting on variable elastic foundation is carried out. The variable elastic foundations include variable Winkler foundation and two-parameter elastic foundation. Linear, parabolic and sinusoidal distributions of Winkler foundation moduli along the axial direction are considered for the analyses. The governing differential equations for beam vibration are being solved using the MDQM. The applied kinematic boundary conditions are implemented using the MWCM. The weighting coefficients are generated from the Chebyshev basis function. The Euler beam theory can be extended for long and thin FGM beams [14] and FG sandwich beams [31]. In the present study, Euler beam displacement distribution theory is considered for the case of single and sandwich beam resting on variable Winkler foundation and two-parameter elastic foundations. The present MDQM results for homogeneous beams on elastic foundations are validated with those available in literature. Present results for vibration of isotropic beam with variable Winkler foundation are in good agreement with those reported in the literature. Effect of (i) temperature distributions, (ii) power-law index, (iii) variable Winkler foundation modulus, (iv) two-parameter elastic foundation modulus and (v) normalized core thickness of FGSW beams on the vibration response of FGM beam and FG sandwich beam are carried out and discussed.

2. Formulations

2.1. FGMs

FGM beam is assumed to be consisting of N equal size layers in the thickness direction. Each layer is considered to be in a plane stress state. The principal direction coincides with the 1 and 2 directions. The corresponding thermo-elastic constitutive law for the kth layer is expressed as

$$\begin{Bmatrix} \sigma_1 \\ \sigma_2 \\ \sigma_6 \end{Bmatrix}^k = \begin{bmatrix} Q_{11} & Q_{12} & 0 \\ Q_{21} & Q_{22} & 0 \\ 0 & 0 & Q_{66} \end{bmatrix}^k \begin{Bmatrix} \varepsilon_1 \\ \varepsilon_2 \\ \varepsilon_6 \end{Bmatrix}^k - \begin{Bmatrix} \bar{\alpha}\Delta T \\ \bar{\alpha}\Delta T \\ 0 \end{Bmatrix}^k \tag{1}$$

where Q_{ij} are the stiffness of the FGM beam at the kth layer and are given as

$$Q_{11} = \frac{E_{\text{fgm}}}{1 - \nu_{\text{fgm}}^2}, \quad Q_{12} = \frac{\nu_{\text{fgm}} E_{\text{fgm}}}{1 - \nu_{\text{fgm}}^2}, \quad Q_{66} = \frac{E_{\text{fgm}}}{2[1 + \nu_{\text{fgm}}]}, \quad \bar{\alpha} = \frac{E_{\text{fgm}}\alpha}{1 - \nu_{\text{fgm}}} \tag{2}$$

Most of the FGMs are being used in high-temperature environment and their material properties are temperature dependent. A typical material property P_i can be expressed as a function of the environment temperature T [3]:

$$P_i = P_0(P_{-1}T^{-1} + 1 + P_1 T + P_2 T^2 + P_3 T^3) \tag{3}$$

where P_0, P_{-1}, P_1, P_2 and P_3 are temperature coefficients and are constants for a specific FGM constituent material. The material property P_{fgm} of FGM is controlled by volume fractions V_{fi} and individual material properties P_i of the constituent materials [3]:

$$P_{\text{fgm}} = \sum_{i=1}^{\text{nm}} P_i V_{\text{fi}} \tag{4}$$

In the present case, two different materials (nm = 2) are particle mixed to form the FGM material. Assuming there are no voids and no foreign particles in the FGM material, sum of the volume fractions of all the constituent materials is unity:

$$\sum_{i=1}^{\text{nm}} V_{\text{fi}} = 1 \tag{5}$$

For example, metal and ceramic materials (nm = 2) are mixed to form the FGM beam. Volume fractions of metal V_m and ceramic V_c materials are defined as

$$V_m = \left(\frac{h-2z}{2h}\right)^{\mathrm{Rn}}, \quad -h/2 \leqslant z \leqslant h/2$$
$$V_c = 1 - V_m \tag{6}$$

where z and h represents the thickness coordinate and the thickness of the beam, respectively. The term Rn denotes the power-law index ($0 \leqslant R_n \leqslant \infty$). Here, volume fraction of the metal material V_m varies from 100% to 0% as z varies from $-h/2$ to $h/2$. Similarly volume fraction of the ceramic material V_c varies from 0% to 100% as z varies from $-h/2$ to $h/2$. For various Rn values, the average volume fractions of metal V_m and ceramic V_c materials are depicted in Ref. [3]. Young's modulus, density, Poisson's ratio and coefficient of thermal conductivity of FGM beam made up of two different materials are expressed as

$$E_{\mathrm{fgm}} = (E_2 - E_1)\left(\frac{2z+h}{2h}\right)^{\mathrm{Rn}} + E_1$$
$$\rho_{\mathrm{fgm}} = (\rho_2 - \rho_1)\left(\frac{2z+h}{2h}\right)^{\mathrm{Rn}} + \rho_1$$
$$v_{\mathrm{fgm}} = (v_2 - v_1)\left(\frac{2z+h}{2h}\right)^{\mathrm{Rn}} + v_1$$
$$k_{\mathrm{fgm}} = (k_{T2} - k_{T1})\left(\frac{2z+h}{2h}\right)^{\mathrm{Rn}} + k_{T1} \tag{7}$$

2.2. FGM beam

In the present work, Euler–Bernoulli beam theory (EBT) for FGM beam is considered [14]. Thus, the beam thickness is assumed to be small and the shear deformation contribution is being neglected. It is assumed that the plane sections normal to the beam axis remain normal and plane after deformation. Furthermore, it is assumed that the thickness of the beam remains unchanged, i.e. displacement w is independent of z. The EBT is based on the displacement

$$u(x,z,t) = u_0(x,t) - z\frac{\partial w}{\partial x}, \quad v = 0, \quad w(x,z,t) = w(x,t) \tag{8}$$

where u_0 and w denote the in-plane and transverse displacements, respectively. The non-zero strains of the Euler–Bernoulli theory are

$$\varepsilon_{xx} = \frac{\partial u_0}{\partial x} - z\frac{\partial^2 w}{\partial x^2} = \varepsilon_0 + zk, \quad \varepsilon_0 = \frac{\partial u_0}{\partial x}, \quad \kappa = -\frac{\partial^2 w}{\partial x^2} \tag{9}$$

where ε_0 and κ is the extensional strain and bending strain, respectively. The stress in the axial direction is written as

$$\sigma_{xx} = \frac{E_{\mathrm{fgm}}}{1 - v_{\mathrm{fgm}}^2}, \quad \varepsilon_{xx} = \frac{E_{\mathrm{fgm}}}{1 - v_{\mathrm{fgm}}^2}(\varepsilon_0 + z\kappa) \tag{10}$$

In the absence of thermal components due to the boundary condition, the axial force and the bending moment resultants for a slender beam are expressed as [14]

$$(N, M) = \int_{-h/2}^{h/2} \frac{E(z)_{\mathrm{fgm}}}{1 - v(z)_{\mathrm{fgm}}^2}\left(\varepsilon_0 - z\frac{\partial^2 w}{\partial x^2}\right)(1, z)\,\mathrm{d}z \tag{11}$$

The relation between the force and moment resultants and the beam deformation is written as

$$\begin{Bmatrix} N \\ M \end{Bmatrix} = \begin{bmatrix} A_{\mathrm{fgm}} & B_{\mathrm{fgm}} \\ B_{\mathrm{fgm}} & D_{\mathrm{fgm}} \end{bmatrix} \begin{Bmatrix} \varepsilon_0 \\ \kappa \end{Bmatrix} \tag{12}$$

where $A_{\rm fgm}$, $B_{\rm fgm}$, $D_{\rm fgm}$ are the in-plane, bending–stretching coupling, bending stiffness of the FGM beam, respectively, and is written as [3]

$$(A_{\rm fgm}, B_{\rm fgm}, D_{\rm fgm}) = \int_{-(h/2)}^{h/2} \left((Q_c - Q_m)\left(\frac{2z+h}{2h}\right)^n (1, z, z^2) + Q_m(1, z, z^2) \right) {\rm d}z \tag{13}$$

where Q_c and Q_m are the elastic stiffness of the FGM constituent material (viz. ceramic and metal).

The Euler–Lagrange equations in $0<x<L$ can be obtained as

$$\frac{\partial N}{\partial x} + f = \rho A \frac{\partial^2 u}{\partial t^2} \tag{14}$$

$$\frac{\partial^2 M}{\partial x^2} + q - \frac{\partial}{\partial x}\left(\bar{N}\frac{\partial w}{\partial x}\right) = \rho A \frac{\partial^2 w}{\partial t^2} - \rho I \frac{\partial^4 w}{\partial x^2 \partial t^2}, \quad 0<x<L \tag{15}$$

The constitutive relation is given as

$$M = B_{\rm fgm}\varepsilon_0 + D_{\rm fgm}\kappa \tag{16}$$

Assuming that there is no in-plane displacement: $u_0 = 0$, $M = D_{\rm fgm}\kappa = -D_{\rm fgm}(\partial^2 w/\partial x^2)$. Substituting M in Eq. (15), we have the governing equation as

$$-D_{\rm fgm}\frac{\partial^4 w}{\partial x^4} + q - \frac{\partial}{\partial x}\left(\bar{N}\frac{\partial w}{\partial x}\right) = \rho A \frac{\partial^2 w}{\partial t^2} - \rho I \frac{\partial^4 w}{\partial x^2 \partial t^2}, \quad 0<x<L \tag{17}$$

2.3. FGM beam on variable elastic foundation

For FGM beam on variable two-parameter elastic foundation [33], the governing equation can be expressed as

$$-D_{\rm fgm}\frac{\partial^4 w}{\partial x^4} + \frac{\partial}{\partial x}\left(k_1(x)\frac{\partial w}{\partial x}\right) - k(x)w + \rho I \frac{\partial^4 w}{\partial x^2 \partial t^2} - \rho A \frac{\partial^2 w}{\partial t^2} = 0, \quad 0<x<L \tag{18}$$

where $k(x)$, $k_1(x)$ are Winkler foundation modulus and second parameter foundation modulus. For analysis of the natural frequency, the above equation is formulated as an eigenvalue problem by assuming the following periodic function:

$$w(x,t) = W(x){\rm e}^{-{\rm i}\omega t} \tag{19}$$

where $W(x)$ is the mode shape of the transverse motion of the beam. Substituting Eq. (19) into Eq. (18) one obtains

$$D_{\rm fgm}\frac{{\rm d}^4 W}{{\rm d}x^4} - \frac{\rm d}{{\rm d}x}\left(k_1(x)\frac{{\rm d}W}{{\rm d}x}\right) + k(x)W - \rho I\omega^2\frac{{\rm d}^2 W}{{\rm d}x^2} + \rho A\omega^2 W = 0, \quad 0<x<L \tag{20}$$

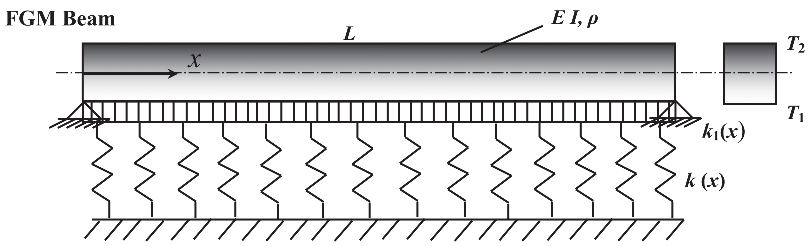

Fig. 1. FGM beam supported on variable two-parameter elastic foundation with simply supported–simply supported ends.

2.4. FGSW beam on variable elastic foundation

A FGSW beam is considered (Fig. 3). The bottom face consists of FGM-I and the top face consists of FGM-II. The core is assumed to be made up of Alporas foam. FGM-I consists of stainless steel and silicon nitride while FGM-II consists of nickel and aluminum oxide. The sandwich beam is maintained in such a way that one surface consists of pure ceramic and the other surface is of fully metal as shown by the shaded diagram. The blackish and whitish shade indicates the presence of ceramic and metal, respectively. The material properties of the constituent material are listed in Tables 1 and 2. The sandwich beam is considered to be resting on variable Winkler foundation (viz. on linear, parabolic and sinusoidal Winkler modulus). In this present case, the effect of second parameter modulus is neglected.

2.5. Temperature distribution

In the present analysis, FGM beam and FGSW beam are considered. The metal and the ceramic surfaces of the beams are considered to be at different temperatures. The variation of temperatures is assumed to be in thickness directional only. One-dimensional steady-state heat conduction along the beam thickness is considered. The temperature distribution $T = T(z)$ is given by the following governing differential equation [32]:

$$\frac{\mathrm{d}}{\mathrm{d}z}\left[k_T(z)\frac{\mathrm{d}T(z)}{\mathrm{d}z}\right] = 0, \quad T(h/2) = T_2, \quad T(-h/2) = T_1 \tag{21}$$

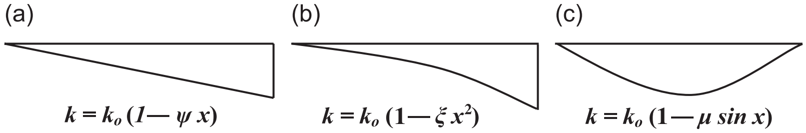

Fig. 2. Various distribution of Winkler elastic foundation along the axial direction: (a) linear type, (b) parabolic type and (c) sinusoidal type.

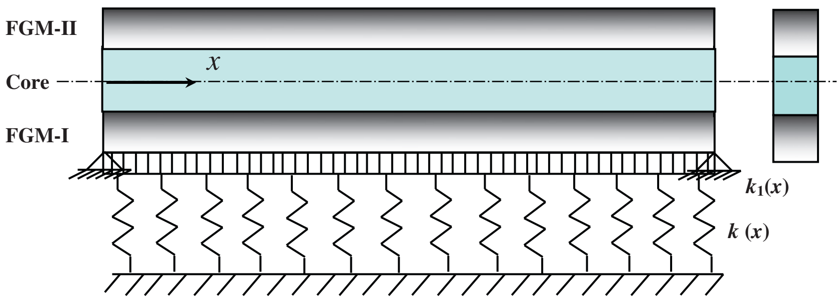

Fig. 3. FGM sandwich beam supported on variable two-parameter elastic foundation with simply supported–simply supported ends.

Table 1
Mechanical and thermal properties of constituent materials of the FGM-I

	Stainless steel (SUS304)				Silicon nitride (Si_3N_4)			
	E	ν	k_T	ρ	E	ν	k_T	ρ
P_0	201.04×10^9	0.3262	15.379	8166.0	348.43×10^9	0.2400	13.723	2370
P_{-1}	0	0	0	0	0	0	0	0
P_1	3.079×10^{-4}	-2.002×10^{-4}	-1.264×10^{-3}	0	-3.070×10^{-4}	0	-1.032×10^{-3}	0
P_2	-6.534×10^{-7}	3.797×10^{-7}	2.092×10^{-7}	0	2.160×10^{-7}	0	5.466×10^{-7}	0
P_3	0	0	-7.223×10^{-10}	0	-8.946×10^{-11}	0	-7.876×10^{-11}	0

Table 2
Mechanical and thermal properties of constituent materials of the FGM-II

	Nickel				Aluminium oxide (Al_2O_3)			
	E	v	k_T	ρ	E	v	k_T	ρ
P_0	223.95×10^9	0.31	58.754	8908.0	349.55×10^9	0.26	-14.087	3750.0
P_{-1}	0	0	0	0	0	0	-1123.6	0
P_1	-2.794×10^{-4}	0	-4.614×10^{-4}	0	-3.853×10^{-4}	0	-6.227×10^{-3}	0
P_2	3.998×10^{-9}	0	6.670×10^{-7}	0	4.027×10^{-7}	0	0	0
P_3	0	0	-1.523×10^{-10}	0	-1.673×10^{-10}	0	0	0

where T_2 and T_1 are the temperature at the top surface and bottom surface, respectively. The solution of the above equation is given in the following form [32]:

$$T(z) = T_1\left(1 + (T_r - 1)\int_{-h/2}^{z}\frac{1}{k(\lambda)}\mathrm{d}\lambda \Bigg/ \int_{-h/2}^{h/2}\frac{1}{k(z)}\mathrm{d}z\right) \tag{22}$$

$$T_r = \frac{T_2}{T_1}$$

T_r is defined as the ratio of the top temperature surface to the bottom surface temperature.

2.6. DQM

In the DQM partial derivatives of a function with respect to a space variable at a given interpolation point is approximated as a weighted linear summation of function values at all chosen interpolation points. Thus, DQM transforms the governing differential equation into a set of equivalent simultaneous equations. This is done by replacing the partial derivative with equivalent weighting coefficients. For example, the first partial derivative is equivalent to a matrix [25]

$$\frac{\partial}{\partial x} \equiv [A]_x \tag{23}$$

Similarly, second-, third- and fourth-order partial derivative are expressed as [25]

$$\begin{aligned}\frac{\partial^2}{\partial x^2} &\equiv [B]_x = [A]_x[A]_x\\ \frac{\partial^3}{\partial x^3} &\equiv [C]_x = [A]_x[A]_x[A]_x\\ \frac{\partial^4}{\partial x^4} &\equiv [D]_x = [A]_x[A]_x[A]_x[A]_x\end{aligned} \tag{24}$$

In the present analyses MDQM is employed. The true implementation of this MDQM technique depends on how accurately the weighting coefficient matrix is computed and the distribution of interpolation points. Unlike the GDQ method, in this modified method (MDQM), weighting coefficients matrix of the first-order derivative is defined by a following matrix multiplication operation [25]

$$[A]_x \equiv [N_0'][N_0]^{-1} \tag{25}$$

where $[N_0]$ is a matrix developed from Chebyshev polynomials of first kind [29] and is defined as

$$N_{0\ (\text{Chebyshev})} = \begin{bmatrix} T_1(x_1) & T_2(x_1) & T_3(x_1) & \cdots & \cdots & T_{n-1}(x_1) & T_n(x_1) \\ T_1(x_2) & T_2(x_2) & T_3(x_2) & \cdots & \cdots & T_{n-1}(x_2) & T_n(x_2) \\ T_1(x_3) & T_2(x_3) & T_3(x_3) & \cdots & \cdots & T_{n-1}(x_3) & T_n(x_3) \\ \vdots & \vdots & \vdots & \vdots & \vdots & \vdots & \vdots \\ \vdots & \vdots & \vdots & \vdots & \vdots & \vdots & \vdots \\ T_1(x_{n-1}) & T_2(x_{n-1}) & T_3(x_{n-1}) & \cdots & \cdots & T_{n-1}(x_{n-1}) & T_n(x_{n-1}) \\ T_1(x_n) & T_2(x_n) & T_3(x_n) & \cdots & \cdots & T_{n-1}(x_n) & T_n(x_n) \end{bmatrix} \tag{26}$$

where, $x_1, x_2, x_3, \ldots, x_n$ are the interpolation points in the computational domain. The components of the Chebyshev polynomials T of first kind are defined as

$$T_1(x_i) = 1,\ \ T_2(x_i) = x_i,\ \ T_2(x_i) = -1 + 2x_i^2,\ \ T_3(x_i) = -3x_i + 4x_i^3 \ldots \tag{27}$$

For choosing interpolation points, one simple way is to divide the computational domain into equal spaces. However, Chen et al. [25] observed that uniform spacing among the interpolation points did not resulted in accurate results. Pradhan and Murmu [29] found that accurate and stable results are being obtained by employing Chebyshev–Gauss–Lobatto interpolation points. Thus, in the present study, these interpolation points are being considered. Locations of these interpolations are determined as follows:

$$x_i = \frac{1}{2}\left[1 - \cos\frac{(i-1)\pi}{(n-1)}\right], \quad i = 1,2,\ldots,n,\ \ 0 \leqslant x_i \leqslant 1 \tag{28}$$

where n is the number of interpolation points. The governing differential equation for a uniform beam with two-parameter elastic foundation is discretized by DQM as

$$D_{\text{fgm}} \sum_{j=1}^{n} D_{ij} W_j - (k_1)_i \sum_{j=1}^{n} B_{ij} W_j + k_i W_i - \rho I \omega^2 \sum_{j=1}^{n} B_{ij} W_j + \rho A \omega^2 W_i = 0, \quad i,j = 1,2,\ldots,n \tag{29}$$

where B_{ij}, D_{ij} are the components of matrix $[B]$ and $[D]$ matrices as expressed in Eq. (8). While imposing various boundary conditions the MWCM approach [27] is employed. In MWCM approach, the boundary conditions are being imposed during the computation of weighting coefficient matrix for inner interpolation points. For simply supported–simply supported case $w = 0$ at $x = 0$ and $x = L$. This leads to elements of first and last columns being replaced by zeros:

$$A_{i1} = 0,\ \ A_{in} = 0, \quad i = 1,2,\ldots,n \tag{30}$$

Thus, A_{ij} is updated as $\bar{A}_{ij}$ where $i,j = 1,2, \ldots, n$. The second-order weighting coefficients is thus written as

$$\bar{B}_{ij} = A_{ik}\bar{A}_{kj}, \quad i,j = 1,2,\ \ldots,\ n \tag{31}$$

During the formulation of third-order derivative coefficient matrix for simply supported–simply supported case, the boundary conditions, $w'' = 0$ at $x = 0$ and $x = L$ are implemented. Similarly, third- and fourth-order weighting coefficients are computed as

$$\begin{aligned} \bar{C}_{ij} &= \bar{A}_{ik}\bar{B}_{kj} \\ \bar{D}_{ij} &= A_{ik}\bar{C}_{kj}, \quad i,j = 1,2,\ \ldots,\ n \end{aligned} \tag{32}$$

The other types of boundary conditions are also implemented in the similar way. The equations are solved for inner grid points. Thus, the differential quadrature analogous with appropriate boundary condition is expressed as

$$D_{\text{fgm}} \sum_{j=2}^{n-1} \bar{D}_{ij} W_j - (k_1)_i \sum_{j=2}^{n-1} \bar{B}_{ij} W_j + k_i W_i - \rho I \omega^2 \sum_{j=2}^{n-1} \bar{B}_{ij} W_j + \rho A \omega^2 W_i = 0 \quad i,j = 2,\ \ldots,\ n-1 \tag{33}$$

Eq. (33) with boundary condition consists of ($n-2$) by ($n-2$) matrix. The above equation can easily be transformed into eigenvalue problem from where the natural frequencies for FGM beam are obtained:

$$[K]\{W\} = \omega^2\{W\} \tag{34}$$

3. Results and discussion

3.1. Validation

3.1.1. Nonlinear variation of Winkler elastic foundation

A simply supported–simply supported isotropic beam resting on nonlinearly varying Winkler modulus is considered. The Winkler elastic modulus is assumed to be varying in a parabolic manner, i.e. $k = k_0\,(1-\xi x^2)$ [19]. In this study, the value of parabolic variation parameter, ξ is varied from 0.2 to 0.8. Winkler elastic constant k_0 is assumed to be 2000. The non-dimensional vibration frequency $\beta = \sqrt[4]{\rho A L^4 \omega^2 / EI}$ as presented in Zhou [19] is computed for first three modes. First three vibration modes' results are plotted in Figs. 4–6, respectively. From these figures, one could observe that present MDQM results for the beam problem do agree well with those reported Zhou [19].

3.1.2. Two-parameter elastic foundation

With the present MDQM, vibration response of a simply supported–simply supported isotropic beam resting on two-parameter elastic foundation is computed. The second parameter modulus k_1 is assumed to be unity. While Winkler modulus is considered to vary from 10 to 100,000. The non-dimensional vibration frequency $\bar{\omega} = \omega L^2 \sqrt{\rho A / EI}$ for first mode is calculated and results are depicted in Fig. 7. From this figure, one could observe that the present MDQM results for the beam analysis are in good agreement with those reported by Matsunaga [22].

3.2. Convergence study

A FG beam (FGM-I) is assumed to be resting on a linearly varying Winkler elastic foundation. The metal-rich surface of the beam is considered to be at room temperature. While the ceramic-rich surface of the FGM

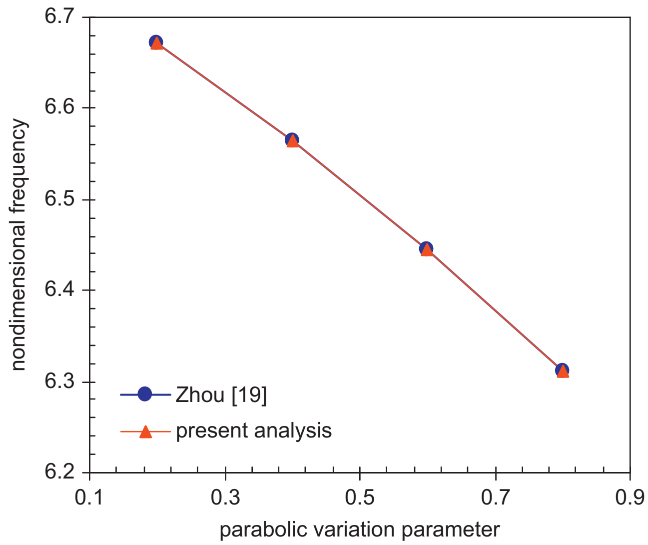

Fig. 4. Comparison of nondimensional frequency β against parameter ξ considering parabolic distribution of Winkler foundation for the first mode of vibration.

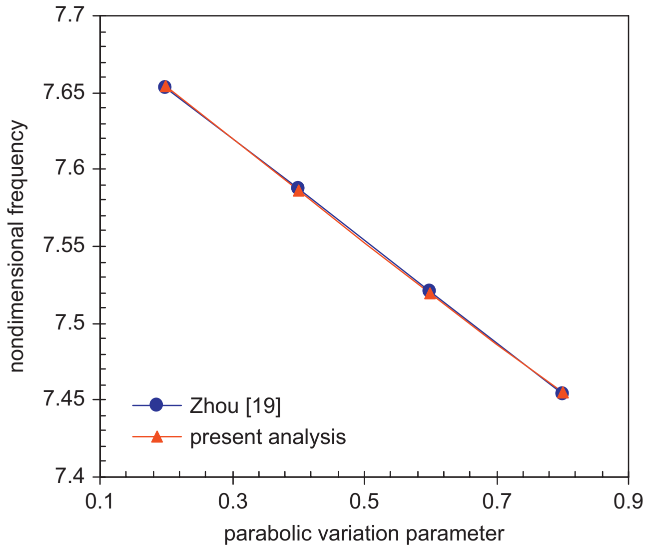

Fig. 5. Comparison of nondimensional frequency β against parameter ξ considering parabolic distribution of Winkler foundation for the second mode of vibration.

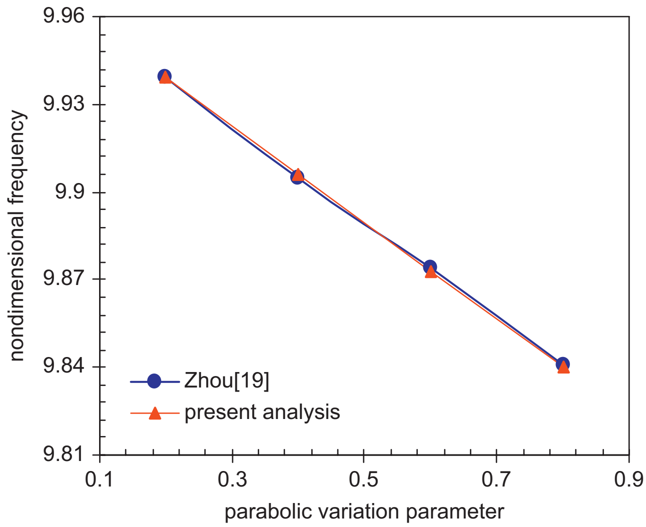

Fig. 6. Comparison of non-dimensional frequency β against parameter ξ considering parabolic distribution of Winkler foundation for the third mode of vibration.

beam is maintained at 1500 K (Fig. 1). Employing the present MDQM, vibration analysis is performed for various power-law indices and with various numbers of interpolation points. The natural frequency versus number of interpolation points for various power-law indices Rn are being plotted in Fig. 8. The results for the natural frequencies are normalized to the form $\bar{\omega} = \sqrt[4]{\bar{\rho} A L^4 \omega^2 / \bar{E} I}$. Here, $\bar{\rho}$ and $\bar{E}$ represent density and elastic modulus, respectively, at room temperature and $\mathrm{Rn} = 0$. In this figure, one could notice that non-dimensional frequency increases rapidly from 3 to 5 interpolation points. Furthermore, non-dimensional frequency converges at 5 and more interpolation points. This trend is observed for power-law index varying from 0.1 to 10. The computational work for the FGM and sandwich beams is conducted employing 11 interpolation points.

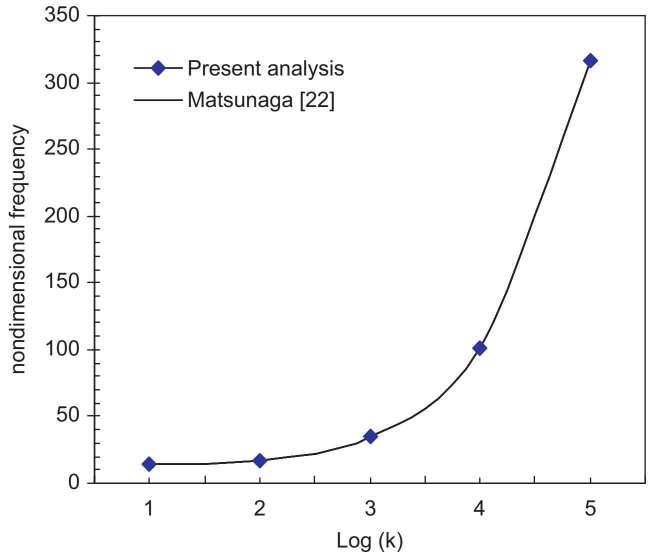

Fig. 7. Comparison of non-dimensional frequency for the first mode for a thin-walled isotropic beam supported on two-parameter elastic foundation.

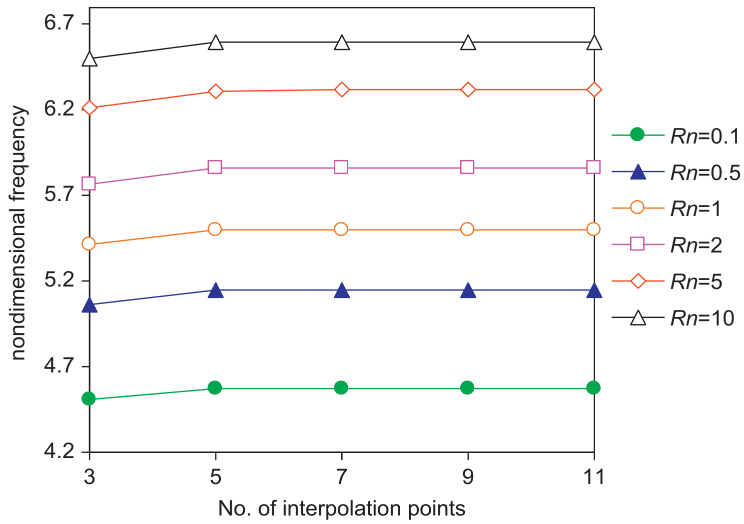

Fig. 8. Convergence of non-dimensional frequency results for different power-law index, Rn, calculated at room temperature.

3.3. Effect of variable Winkler elastic foundation

MDQM analysis is extended to a simply supported–simply supported FGM beam resting on Winkler elastic foundation. The beam is assumed to be made up of FGM-I material as mentioned in Table 1. The FGM-I beam consists of silicon nitride (Si_3N_4) and stainless steel (SUS304) materials, which are commonly used materials for FGMs in the literature. The beam is considered to be resting on various Winkler elastic foundations. These include linear-, parabolic- and sinusoidal-type variations along the axial direction (Fig. 2).

Effect of various parameters on the natural frequency is being studied. These parameters include (a) different types of Winkler elastic foundation (Fig. 2), (b) temperature distributions along the thickness direction (Fig. 1) and (c) power-law index Rn of FGM beam. The metal-rich surface of the FGM beam is maintained at room temperature. While the ceramic-rich surface of the beam is exposed to 300, 500, 900 and

1500 K, respectively. The beam deformation is considered to be elastic in nature. The temperature-dependent and spatially dependent material properties of the beam are assumed to vary through the thickness. At constant thickness coordinate value, the temperature is considered to be same in the entire two-dimensional plane.

The temperature variation along the thickness is computed as per Eqs. (21) and (22). The temperature variation of FGM-I beam across the thickness is found to be almost same for the values of power-law indices Rn, considered in the analysis. This behavior is found for various sets of top and bottom surface temperatures considered. This is due to the fact that the ratio of thermal conductivities of these two materials of FGM-I is close to unity. However, for high value of thermal conductivity ratio the temperature variations across the thickness are significantly different with different Rn values.

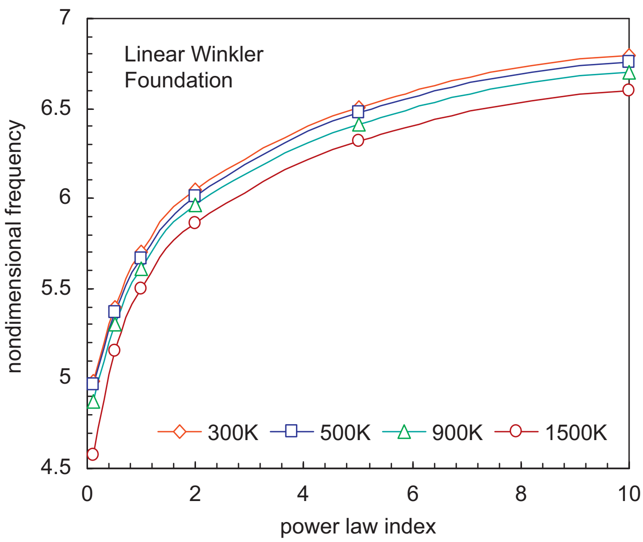

Fig. 9. Variation of non-dimensional frequency with power-law index, Rn, at different temperatures of ceramic-rich surface of FGM beam with linear Winkler foundation.

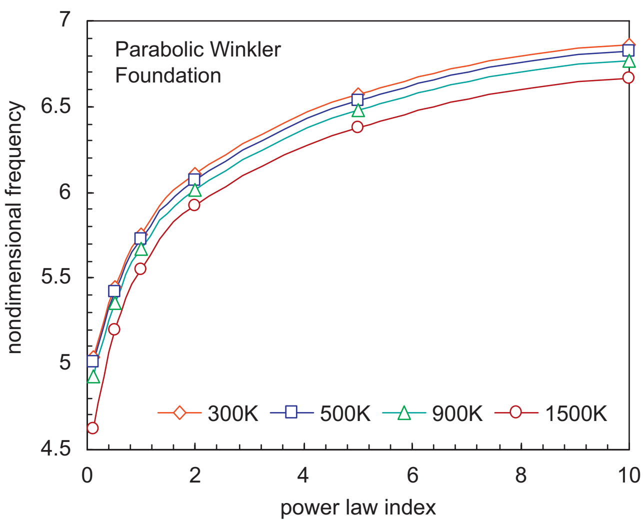

Fig. 10. Variation of non-dimensional frequency with power-law index, Rn, at different temperatures of ceramic-rich surface of FGM beam with parabolic Winkler foundation.

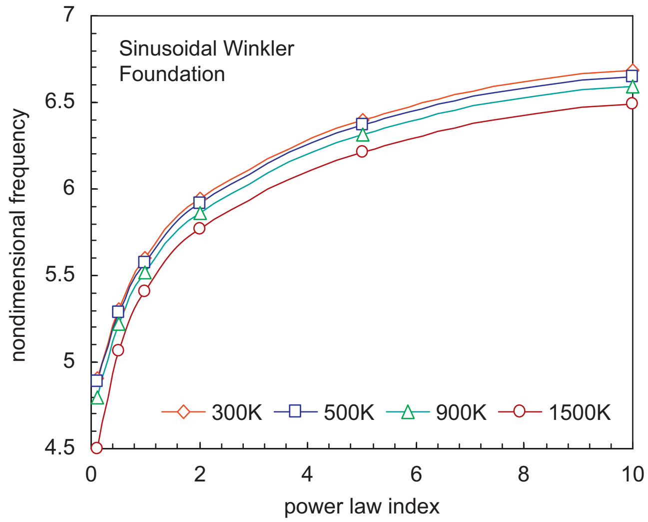

Fig. 11. Variation of non-dimensional frequency with power-law index, Rn, at different temperatures of ceramic-rich surface of FGM beam with sinusoidal Winkler foundation.

Figs. 9–11 show the variation of non-dimensional fundamental frequency versus power-law indices Rn for various temperature distributions. The temperature distributions were due to application of different temperatures on the purely ceramic surface. From these three figures, it is seen that the non-dimensional fundamental frequency increases as the power-law indices Rn increase. This increase in frequency with power-law index is attributed to the fact that silicon nitride has larger stiffness than that of stainless steel. When the value of power-law index, Rn, is zero, FGM beam consists of only stainless steel. Thus, frequency value is least when Rn is zero. With increase of Rn value, the more ceramic materials are included in the FGM beam.

Furthermore, the value of non-dimensional fundamental frequency increases rapidly for power-law indices Rn varying from 0.1 to 2. While the frequency value increases marginally for power-law indices Rn varying from 2 to 10. This is due to the fact that for power-law index varying from 0.1 to 2, more percentage of ceramic material is present in the FGM beam. While for power-law index varying from 2 to 10 the FGM beam becomes ceramic rich.

The non-dimensional fundamental frequency is also observed to change with application of high temperature on the ceramic rich surface of the FGM beam (Fig. 1). With increase of temperature, the non-dimensional fundamental frequencies decrease. This is because the material properties are dependent on temperature (Eq. (3)). As higher temperature is applied on the ceramic-rich surface, the stiffnesses of the constituent materials of FGM beam are decreased.

The variation of non-dimensional fundamental frequency with power-law indices Rn for linear, parabolic and sinusoidal variations of Winkler foundation are plotted in Figs. 9–11, respectively. For all these three cases, the frequencies decrease as the temperature increases. From Figs. 9 to 11, it is observed that non-dimensional fundamental frequency versus power-law index Rn variation for all the three cases are similar in nature. However, from Fig. 12, one could observe that non-dimensional fundamental frequencies for the linear, parabolic and sinusoidal variations of Winkler foundation are significantly different. For this comparative study, Rn and $k_{\max}$ are assumed to be 1 and 500, respectively. The value of fundamental frequency increases with inclusion of elastic foundation. From this figure, it is found that parabolic variation of the Winkler elastic foundation yielded larger non-dimensional frequency value as compared with linear and sinusoidal variations. One could note that there is a rise in frequency values of FGM beam when the stiffness of Winkler elastic foundation is more in one of the two boundaries.

Linear variation of the Winkler elastic foundation yielded larger non-dimensional frequency value as compared with non-dimensional frequency value of sinusoidal variation. This is because the stiffness of linear variation of the Winkler elastic foundation is more near one of the supports. While stiffness of sinusoidal variation of the Winkler elastic foundation is more near the mid-span. From the present study, one could infer

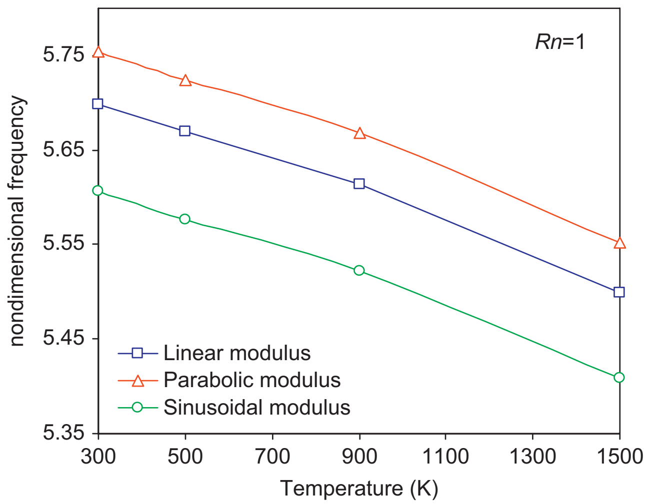

Fig. 12. Variation of non-dimensional frequency with increase in temperature of ceramic rich surface of FGM beam with various Winkler foundations. Power-law index is considered as unity.

that parabolic variation of Winkler foundation should be employed for obtaining larger natural frequency in the FGM beam design.

3.4. Effect of two-parameter elastic foundation

Vibration response of FGM beam resting on two-parameter elastic foundation is studied. The metal-rich surface of the FGM beam (Fig. 1) is maintained at room temperature. While the ceramic-rich surface of the beam is exposed to 300, 500, 900, 1100 and 1500 K, respectively. The temperature-dependent and spatially dependent material properties of the beam are assumed to vary through the thickness. At constant thickness coordinate value, the temperature is assumed to be same in the entire two-dimensional plane.

Results of non-dimensional frequencies for various combinations of Winkler elastic modulus k and second parameter k_1 are listed in Tables 3 and 4. In present analysis, Winkler elastic modulus, k is assumed to be 10. Second parameter elastic foundation modulus k_1 is considered to be 2, 5, 10 and 50, respectively. Simply supported–simply supported and clamped–simply supported boundary conditions are included in the computation.

From Tables 3 and 4, one could observe that non-dimensional fundamental frequency increases with the increase of power-law index Rn and decreases with increase of applied temperature. Non-dimensional fundamental frequency also increases as one increase the second parameter elastic modulus k_1. This is due to the fact that stiffness of foundation contributes to the increase of non-dimensional fundamental frequency. However, the influence of stiffness of Winkler elastic foundation on frequency is stronger as compared with that of second parameter elastic foundation.

It is interesting to note that second parameter elastic modulus k_1 has stronger effect on non-dimensional fundamental frequency as compared with effects of power-law index and applied temperature. Thus, non-dimensional fundamental frequency could be achieved with larger second parameter elastic modulus k_1. Furthermore, it is observed that power-law index Rn has stronger influence on fundamental frequency as compared with applied temperature.

Furthermore, the effect of boundary conditions on the non-dimensional frequency of the FGM beam supported on two-parameter elastic foundation is listed in Tables 3 and 4. Non-dimensional frequency of FGM beam with clamped–simply supported boundary condition is found to be larger than that with simply supported–simply supported boundary condition. However, effect of boundary condition is diminished when high temperatures are applied on ceramic-rich top surface. From Tables 3 and 4, one could also observe that non-dimensional frequency for clamped–simply supported boundary condition is 25% more than that of

Table 3
Non-dimensional frequency for simply supported–simply supported boundary condition on two-parameter elastic foundation with different temperatures of ceramic-rich surface of FGM beam ($k = 10$)

k_1	Rn	Room temperature	300 K	500 K	900 K	1100 K	1500 K
2	0.1	4.301	4.300	4.282	4.204	4.140	3.945
	0.5	4.653	4.652	4.630	4.575	4.539	4.438
	1	4.913	4.912	4.887	4.839	4.812	4.740
	2	5.214	5.213	5.185	5.138	5.114	5.053
	5	5.610	5.609	5.580	5.531	5.506	5.446
	10	5.858	5.857	5.827	5.776	5.752	5.690
	50	6.164	6.163	6.132	6.081	6.056	5.994
5	0.1	5.093	5.093	5.071	4.978	4.903	4.672
	0.5	5.511	5.510	5.483	5.417	5.375	5.256
	1	5.819	5.818	5.787	5.731	5.699	5.614
	2	6.174	6.173	6.140	6.085	6.057	5.984
	5	6.644	6.643	6.608	6.550	6.521	6.449
	10	6.938	6.936	6.901	6.841	6.812	6.739
	50	7.300	7.299	7.262	7.201	7.172	7.098
10	0.1	5.915	5.914	5.889	5.782	5.695	5.425
	0.5	6.400	6.399	6.367	6.292	6.242	6.104
	1	6.758	6.756	6.721	6.655	6.618	6.520
	2	7.171	7.169	7.131	7.067	7.034	6.950
	5	7.716	7.715	7.674	7.607	7.573	7.490
	10	8.057	8.056	8.014	7.945	7.911	7.826
	50	8.478	8.477	8.434	8.363	8.329	8.244
50	0.1	8.664	8.663	8.625	8.469	8.341	7.947
	0.5	9.374	9.373	9.326	9.215	9.143	8.941
	1	9.898	9.896	9.845	9.748	9.694	9.549
	2	10.503	10.501	10.445	10.351	10.303	10.180
	5	11.302	11.300	11.241	11.142	11.093	10.970
	10	11.802	11.799	11.738	11.637	11.587	11.463
	50	12.418	12.416	12.353	12.250	12.200	12.075

simply supported–simply supported boundary condition. This is for the case when T, k_1 and Rn are considered to be 300, 2 and 0.1 K, respectively. While this change is just 5% for T, k_1 and Rn are considered to be 1500, 50 and 50 K, respectively. This infers that non-dimensional frequency is a strong function of boundary condition at lower temperature, smaller values of k_1 and smaller values of Rn. This is because of the fact that clamped boundary condition provides more stiffness at lower temperature, smaller k_1 and smaller Rn values.

3.5. *Effect of Rt on frequency of sandwich beam*

Present computational work is extended to the FGSW beam. The bottom and top faces of the FGSW beam are assumed to be of FGM-I and FGM-II, respectively. FGM-I consists of stainless steel and silicon nitride while FGM-II consists of nickel and aluminum oxide. The material properties of the constituent materials of FGM-I and FGM-II are listed in Tables 1 and 2. The core of the FGSW beam is Alporas foam. Young's modulus, Poisson's ratio and density of Alporas foam are assumed to be 0.5 GPa, 0.35 and 0.22 gm/cm^3, respectively. Thicknesses of top and bottom faces of FGSW beam are assumed to be identical. Non-dimensional core thickness ratio, Rt, is defined as the ratio of core thickness to face thickness. The length to thickness ratio is maintained more than 20 such that EBT is applicable [31]. Furthermore, the FGSW beam is considered to be resting on variable Winkler foundation (viz. linear, sinusoidal and parabolic Winkler elastic foundation). Temperatures at various locations of the FGSW beam are shown in Fig. 3. Three sets of applied

Table 4
Non-dimensional frequency for clamped–simply supported boundary condition on two-parameter elastic foundation with different temperatures of ceramic-rich surface of FGM beam ($k = 10$)

k_1	Rn	Room temperature	300 K	500 K	900 K	1100 K	1500 K
2	0.1	4.807	4.807	4.786	4.699	4.628	4.409
	0.5	5.201	5.200	5.175	5.113	5.073	4.961
	1	5.492	5.491	5.462	5.409	5.378	5.298
	2	5.827	5.826	5.796	5.743	5.716	5.648
	5	6.271	6.270	6.237	6.182	6.155	6.087
	10	6.548	6.547	6.513	6.457	6.429	6.360
	50	6.890	6.889	6.854	6.797	6.769	6.700
5	0.1	5.485	5.484	5.461	5.361	5.280	5.031
	0.5	5.934	5.933	5.904	5.834	5.788	5.660
	1	6.266	6.265	6.232	6.171	6.137	6.045
	2	6.649	6.648	6.613	6.553	6.522	6.445
	5	7.155	7.154	7.116	7.053	7.023	6.945
	10	7.471	7.470	7.431	7.367	7.335	7.257
	50	7.861	7.860	7.821	7.755	7.723	7.644
10	0.1	6.233	6.232	6.206	6.093	6.001	5.717
	0.5	6.744	6.743	6.710	6.630	6.578	6.432
	1	7.121	7.120	7.083	7.013	6.974	6.870
	2	7.556	7.555	7.515	7.447	7.412	7.324
	5	8.131	8.130	8.087	8.016	7.981	7.892
	10	8.491	8.489	8.445	8.372	8.336	8.247
	50	8.934	8.932	8.888	8.813	8.777	8.687
50	0.1	8.843	8.842	8.803	8.644	8.513	8.111
	0.5	9.567	9.566	9.519	9.406	9.332	9.125
	1	10.102	10.101	10.048	9.949	9.894	9.746
	2	10.720	10.718	10.661	10.564	10.515	10.390
	5	11.535	11.533	11.473	11.372	11.322	11.197
	10	12.045	12.043	11.981	11.877	11.826	11.700
	50	12.674	12.672	12.608	12.503	12.451	12.324

temperatures (Fig. 3) are included in the present study viz. T (294–294–294), T (294–294–1500) and T (294–1500–294). The number in the parenthesis denotes the temperature in Kelvin.

Effect of various parameters on the vibration response of FGSW beam is examined. These parameters include (a) types of Winkler foundation (viz. linear, parabolic and sinusoidal variation, Fig. 2), (b) core thickness ratio, Rt, (c) temperature variation along the thickness direction and (d) power-law index, Rn. Frequency parameter is defined as $\psi = \sqrt[4]{\omega(\rho A/EI)^2}$.

Fig. 13 shows the variation of frequency parameter for various core thicknesses, Rt. Results related to first five modes of vibration are shown in Fig. 13. The power-law index Rn for the present case is assumed to be 0.1. From this figure, one could observe that with increase in non-dimensional core thicknesses ratio, Rt, frequency parameter decrease. This can be attributed to the fact that when the core thickness ratio increases, the overall flexural rigidity of the FGSW beams increases. It should be noted that frequency parameter is inversely proportional to flexural rigidity. Furthermore, it is interesting to note that this variation of Rt, and frequency parameter for modes 1, 2 and 3 are almost linear in nature. While variation of Rt and frequency parameter is nonlinear in nature for modes 4 and 5.

Fig. 14 shows the effect of power-law index Rn on frequency parameter for various core thicknesses ratios, Rt. From this figure, one could note that with increase in core thicknesses ratios Rt frequency parameter decreases for all power-law indices Rn. Rate of decrease is observed to be independent of applied Rn values. As the Rn value increases the associated frequency parameter increases. When $\mathrm{Rn} = 0$, the FGSW beam consists of purely ceramic top face, core and purely ceramic bottom face. With increase of Rn, more metal is

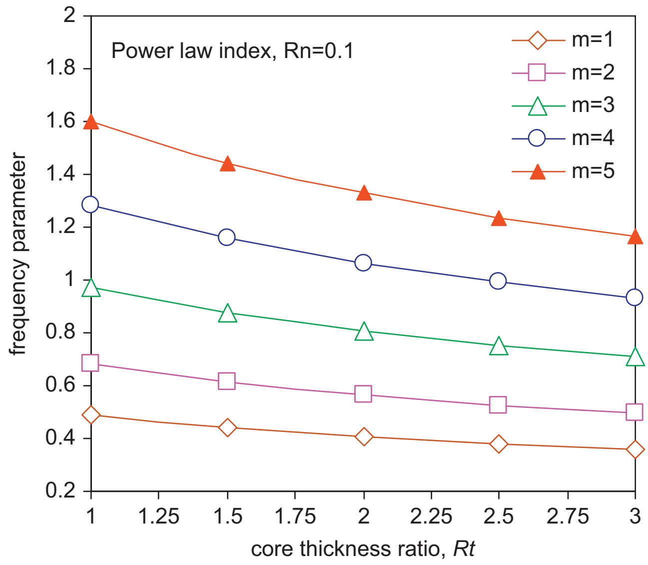

Fig. 13. Variation of frequency parameter with core thickness ratio of (FGM-I core FGM-II) sandwich beam under linearly varying Winkler elastic modulus for different modes; Rn = 0.1.

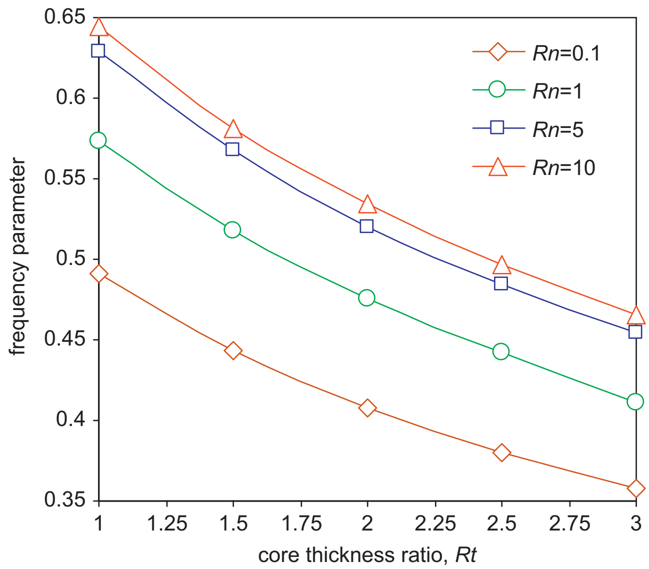

Fig. 14. Variation of frequency parameter with core thickness ratio of (FGM-I core FGM-II) sandwich beam under linearly varying Winkler elastic modulus for different value of power-law indices.

included in the top and bottom faces. Thus, the effective stiffness of the FGSW beam is decreased. And hence larger frequency parameter is observed with larger power-law index values.

Fig. 15 shows the effect of three different Winkler foundations (Fig. 2) on frequency parameter for various core thickness ratios, Rt. For this investigation, Rn is assumed to be unity and same numerical value ($k_{\max} = 500$) in linear, parabolic and sinusoidal variation of Winkler foundation (Fig. 2) is employed. Furthermore, it is observed that parabolic variation of the Winkler elastic foundation yields larger frequency

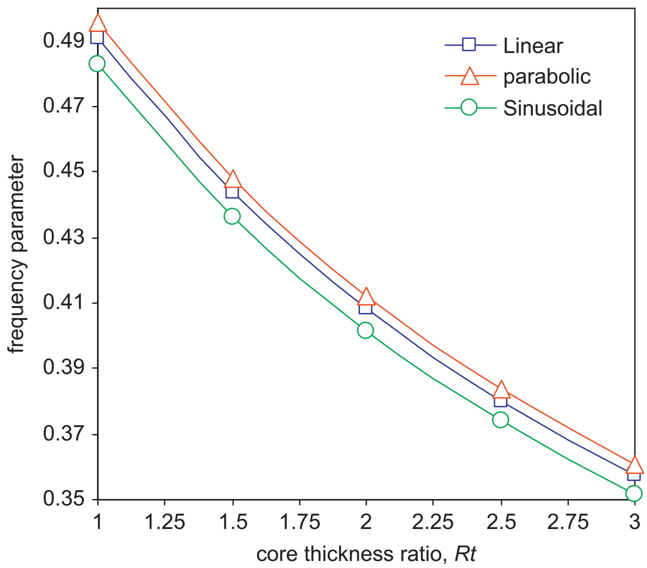

Fig. 15. Variation of frequency parameter with core thickness ratio of (FGM-I core FGM-II) sandwich beam for different variation of Winkler elastic modulus along the axial direction.

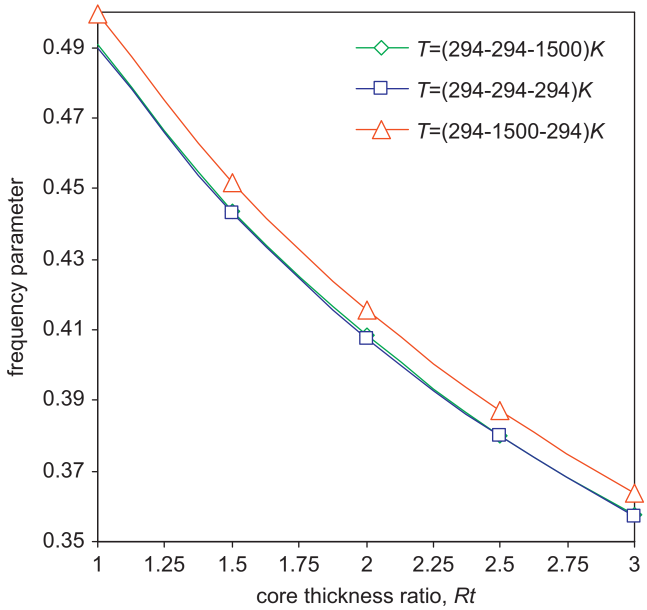

Fig. 16. Comparison of frequency parameter variation against core thickness ratio of (FGM-I core FGM-II) sandwich beam for different temperature distribution; Rn = 0.1.

parameter value as compared with linear and sinusoidal variation. Furthermore, linear variation of the Winkler elastic foundation yields larger frequency parameter value as compared with sinusoidal variation. From these results, one could infer that parabolic variation should be employed for obtaining larger natural frequency in the beam design.

Figs. 16 and 17 show the effect of three different temperature distributions on frequency parameter for various core thickness ratios Rt. These results are for Rn = 0.1 and 10, respectively. From these figures, one could observe that the increase in the temperature of the core material increases the frequency parameter. It is

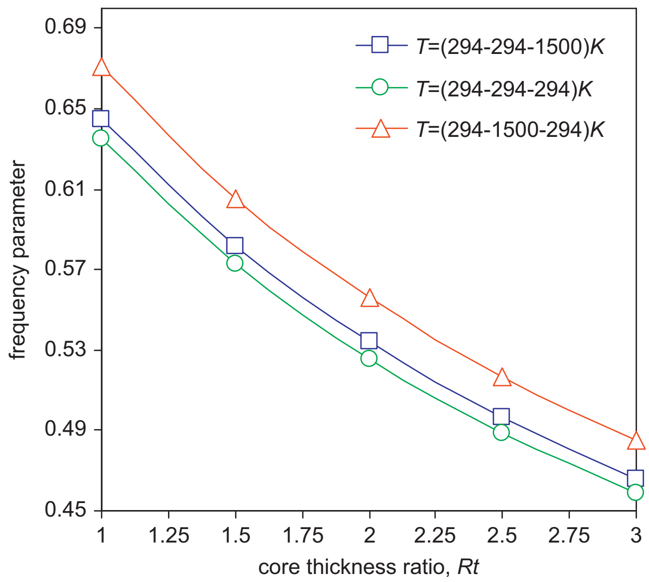

Fig. 17. Comparison of frequency parameter variation against core thickness ratio of (FGM-I core FGM-II) sandwich beam for different temperature distribution; Rn = 10.

observed that for the temperature variation of T (294–1500–294) profile imparts the highest frequency parameter. This can be attributed to the fact that when high temperature is applied to core material, heat is conducted to the top and bottom faces of FGSW beam. As a consequence, the effective stiffness of the FGSW beam is reduced. This effect is more prominent with higher values power-law index Rn.

4. Conclusions

Using MDQM thermo-mechanical vibration analysis of FG beams and FGSW beams are presented. Parametric study on the vibration response of FG beams and FGSW beams are being carried out. These parameters include (i) temperature distributions, (ii) power-law index, (iii) variable Winkler foundation modulus, (iv) two-parameter elastic foundation modulus and (v) normalized core thickness of FGSW beams. Present results for the beam with Winkler and two-parameter elastic foundations do agree with those reported in the literature. Non-dimensional fundamental frequency increase with increase in power-law index Rn. Also, the frequency decreases as the temperature increases. Among linear, parabolic and sinusoidal variation of Winkler foundation, parabolic variation should be employed for obtaining larger natural frequency in the FGM beam design.

For two-parameter elastic foundation non-dimensional frequency increases with increase in second parameter elastic modulus, power-law index and decreases with applied temperature. Second parameter elastic modulus has stronger effect on natural frequency than power-law index and applied temperature. This infers that natural frequency is a strongly influenced by boundary condition at lower temperature, smaller values of k_1 and smaller value of Rn.

For the FGSW beam, frequency parameter decreases with increase in core thicknesses ratios Rt for all power-law indices Rn. Rate of decrease is observed to be independent of applied Rn values. Furthermore, increase in the temperature of the core material increases the frequency parameter. This effect is more prominent when power-law index Rn is order of 10.

Acknowledgement

The financial support of this research work by AR&DB Structures Panel DARO/08/1051321/M/I grant was gratefully acknowledged.

References

[1] M. Koizumi, FGM activities in Japan, *Composites Part B* 28B (1997) 1–4.
[2] Z.F. Shi, Y. Chen, Functionally graded piezoelectric cantilever beam under load, *Archive of Applied Mechanics* 74 (2004) 3–4.
[3] S.C. Pradhan, Vibration suppression of FGM composite shells using embedded magnetostrictive layers, *International Journal of Solids and Structures* 42 (2005) 2465–2488.
[4] S.C. Pradhan, C.T. Loy, K.Y. Lam, J.N. Reddy, Vibration characteristics of functionally graded cylindrical shells under various boundary conditions, *Applied Acoustics* 61 (1) (2000) 111–129.
[5] S. Suresh, A. Mortensen, *Fundamentals of Functionally Graded Materials*, IOM Communications Limited, London, UK, 1998.
[6] G.N. Praveen, J.N. Reddy, Nonlinear transient thermo-elastic analysis of functionally graded ceramic–metal plates, *International Journal of Solids and Structures* 35 (1998) 4457–4476.
[7] J.N. Reddy, Z.Q. Cheng, Three-dimensional solutions of smart functionally graded plates, *Journal of Applied Mechanics* 68 (2) (2001) 234–241.
[8] L. Librescu, S.Y. Oh, O. Song, Thin-walled beams made of functionally graded materials and operating in a high temperature environment: vibration and stability, *Journal of Thermal Stresses* 28 (2005) 649–712.
[9] V. Birman, L.W. Byrd, Modeling and analysis of functionally graded materials and structures, *Applied Mechanics Reviews* 60 (2007) 195–216.
[10] Q. Li, V.P. Iu, K.P. Kou, Three-dimensional vibration analysis of functionally graded material sandwich plates, *Journal of Sound and Vibration* 311 (1–2) (2008) 498–515.
[11] A.M. Zenkour, A comprehensive analysis of functionally graded sandwich plates—part 1: deflection and stresses, *International Journal of Solids and Structures* 42 (18–19) (2005) 5224–5242.
[12] A.M. Zenkour, A comprehensive analysis of functionally graded sandwich plates—part 2: buckling and free vibration, *International Journal of Solids and Structures* 42 (2005) 5243–5258.
[13] S. Venkataraman, B.V. Sankar, Elasticity solution for stresses in a sandwich beam with functionally graded core, *AIAA Journal* 41 (12) (2003) 2501–2505.
[14] B.V. Sankar, An elasticity solution for functionally graded beams, *Composites Science and Technology* 61 (2001) 689–696.
[15] H. Zhu, B.V. Sankar, A combined Fourier series-Galerkin method for the analysis of functionally graded beams, *Journal of Applied Mechanics—Transactions of the ASME* 71 (2004) 421–424.
[16] A. Chakraborty, S. Gopalakrishnan, J.N. Reddy, A new beam finite element for the analysis of functionally graded materials, *International Journal of Mechanical Sciences* 45 (2003) 519–539.
[17] Z. Zhong, T. Yu, Analytical solution of a cantilever functionally graded beam, *Composites Science and Technology* 67 (2007) 481–488.
[18] R.K. Bhangale, N. Ganesan, Thermoelastic vibration and buckling analysis of functionally graded sandwich beam with constrained viscoelastic core, *Journal of Sound and Vibration* 295 (2006) 294–316.
[19] D. Zhou, A general solution to vibrations of beams on variable Winkler elastic foundation, *Computers and Structures* 47 (1) (1993) 83–90.
[20] D. Thambiratnam, Y. Zhuge, Free vibration analysis of beams on elastic foundation, *Computers and Structures* 60 (6) (1996) 971–980.
[21] F.T.K. Au, D.Y. Zheng, Y.K. Cheung, Vibration and stability of non-uniform beams with abrupt changes of cross-section by using C^1 modified beam vibration functions, *Applied Mathematics and Modeling* 29 (1999) 19–34.
[22] H. Matsunaga, Vibration and buckling of deep beam–columns on two-parameter elastic foundations, *Journal of Sound and Vibration* 228 (2) (1999) 359–376.
[23] J. Ying, C.F. Lu, W.Q. Chen, Two-dimensional elasticity solutions for functionally graded beams resting on elastic foundations, *Composite Structures* 84 (2008) 209–219.
[24] R. Bellman, B.G. Kashef, J. Casti, Differential quadrature: a technique for a rapid solution of non linear partial differential equations, *Journal of Computational Physics* 10 (1972) 40–52.
[25] W. Chen, A.G. Striz, C.W. Bert, A new approach to the differential quadrature method for fourth-order equations, *International Journal for Numerical Methods in Engineering* 40 (1997) 1941–1956.
[26] C.W. Bert, S.K. Jang, A.G. Striz, Two new approximate methods for analyzing free vibration of structural components, *AIAA Journal* 26 (1988) 612–618.
[27] X. Wang, C.W. Bert, A new approach in applying differential quadrature to static and free vibrational analyses of beams and plates, *Journal of Sound and Vibration* 162 (1993) 566–572.
[28] C. Shu, H. Du, Implementation of clamped and simply supported boundary conditions in the GDQ free vibration analysis of beams and plates, *International Journal of Solids and Structures* 34 (1996) 819–835.
[29] S.C. Pradhan, T. Murmu, Analysis of FGM sandwich structures with modified differential quadrature method, *Proceedings of the International Conference in Structural Engineering*, Manipal, India, 2007, pp. 119–128.
[30] S.A. Fazelzadeh, P. Malekzadeh, P. Zahedinejad, M. Hosseini, Vibration analysis of functionally graded thin-walled rotating blades under high temperature supersonic flow using the differential quadrature method, *Journal of Sound and Vibration* 306 (2007) 333–348.
[31] Q. Wang, S.T. Quek, Flexural vibration analysis of sandwich beam coupled with piezoelectric actuator, *Smart Materials and Structures* 9 (2000) 103–109.
[32] S.R. Li, J.H. Zhang, Y.G. Zhao, Nonlinear thermomechanical post-buckling of circular FGM plate with geometric imperfection, *Thin-Walled Structures* 45 (2007) 528–536.
[33] M. Eisenberger, Vibration frequencies for beams on variable one and two parameter elastic foundations, *Journal of Sound and Vibration* 176 (5) (1994) 577–584.